Field and temperature dependence of dielectric properties in $BaTiO_3$-based piezoceramics

1998 J. Phys.: Condens. Matter 10 461

(http://iopscience.iop.org/0953-8984/10/2/025)

J. Phys.: Condens. Matter **10** (1998) 461–476. Printed in the UK PII: S0953-8984(98)84804-2

Field and temperature dependence of dielectric properties in $BaTiO_3$-based piezoceramics

D A Hall, M M Ben-Omran and P J Stevenson

Materials Science Centre, University of Manchester and UMIST, Grosvenor Street, Manchester M1 7HS, UK

Received 3 June 1997, in final form 15 September 1997

Abstract. The high-field dielectric properties of a commercial cobalt-doped $BaTiO_3$ piezoceramic were determined by analysis of P–E (polarization–electric field) hysteresis loops. Measurements recorded under a continuous high AC field (amplitude $E_0 = 2$ kV mm^{-1}) established that the material underwent a diffuse ferroelectric phase transformation at a temperature of approximately 100 °C. Gradual increases in the dielectric coefficients ε_r' and ε_r'' were observed on increasing the field amplitude from 0.1 to 0.4 kV mm^{-1}, which were attributed to increased contributions from reversible ferroelectric domain wall vibration. Beyond a certain threshold field level (typically in the range 0.4 to 0.8 kV mm^{-1}), sharp increases in ε_r' and ε_r'' were evident, corresponding to the onset of ferroelectric domain switching. The appearance of a significant internal bias field E_i could also be correlated with the onset of domain switching. A procedure was proposed for determination of the intrinsic (ionic), the ferroelectric domain wall vibration and the domain switching contributions to the dielectric coefficients by analysis of the linear reversible and nonlinear hysteretic components of the measured P–E loops.

1. Introduction

The application of ceramic $BaTiO_3$-based dielectrics in multilayer ceramic capacitors is well documented [1]. Poled $BaTiO_3$ ceramics also find significant applications in piezoelectric devices such as air ranging transducers and low-power SONAR sources [2]. In many of these applications, ferroelectric ceramic materials such as $BaTiO_3$ and PZT (lead zirconate titanate) are subject to high levels of electric field and mechanical stress, under which their dielectric and piezoelectric properties are not well characterized or understood [3]. Therefore, there is an urgent need to provide both an improved description and a theoretical understanding of the behaviour of ferroelectric ceramics under high-field conditions.

The effect of electric field strength on the dielectric properties of ferroelectric ceramics has been of considerable interest since the discovery of ferroelectricity in $BaTiO_3$ in the 1940s. Early observations of ferroelectric hysteresis at high electric field levels ($\sim$1 kV mm^{-1}) were attributed to the formation and mobility of ferroelectric domains in such materials [4]. At lower field strengths in the range 0.1 to 1 kV mm^{-1}, the dielectric loss was attributed to a combination of reversible domain wall oscillations and domain switching, referred to by Lewis as 'microhysteresis' and 'macrohysteresis' effects respectively [5]. It was observed in this work and in subsequent studies [6] that a threshold electric field strength could be identified, below which the hysteretic contributions were negligible.

A number of studies have been published during recent years concerning the high-field behaviour of barium titanate and PZT ceramics, using various measurement methods [7–9].

0953-8984/98/020461+16$19.50

All these authors concluded that the observed increases in dielectric permittivity and loss as a function of field amplitude were a result of increased extrinsic (ferroelectric domain wall) contributions to these coefficients. However, to date few attempts have been made to distinguish between contributions from reversible domain wall motion and the domain switching which is more clearly evident at high field levels.

The present work was carried out to provide an improved description of the high-field dielectric properties of $BaTiO_3$-based piezoceramics, as part of a wider study of ageing effects in acceptor-doped ferroelectric ceramics. During the course of the work, it became evident that a number of important dielectric parameters could be determined by analysis of the evolution of the measured P–E loops as a function of field amplitude; therefore, the implications of this method for determination of the domain-related contributions to the complex permittivity ε_r^* are examined in some detail.

2. Experimental procedures

The subject of the present work was a commercial cobalt-doped $BaTiO_3$ piezoceramic, type PC3, manufactured by Morgan Matroc (Unilator Division, Ruabon, UK). The material was obtained from the manufacturer as a calcined powder, in a spray-dried granular form. A 12 mm uniaxial steel die was employed to produce green pellets from this powder, using a pressure of 100 MPa. The pressed pellets were subsequently sintered for 1.5 hours in air at a temperature of 1400 °C. Specimens for electrical testing were prepared by applying a silver-loaded paste (DuPont type 7095), which was fired on at 550 °C to achieve a conductive and adherent coating.

The crystal structure of the sintered ceramics was assessed by XRD using a Philips APD system employing Cu Kα radiation, while the microstructure was examined using a Philips SEM505. Low-field dielectric measurements were carried out as a function of temperature using a Hewlett Packard HP4284A *LCR* meter in combination with a wire-wound alumina tube furnace. Electrical contact to the specimen was established by means of Pt wire and foil electrodes. The measurements were conducted on heating at a rate of 1 °C min^{-1}, with values of capacitance and dielectric loss being recorded at temperature intervals of 1 °C.

High-field dielectric measurements were conducted using a TG1304 computer-controlled function generator (Thurlby–Thandar) in conjunction with a HVA1B high-voltage ($\times$1000) amplifier (Chevin Research, Otley, UK). A two-probe brass specimen holder was immersed in a temperature-controlled silicone oil bath in order to obtain a stable ($\pm$0.5 °C) temperature environment for the experiments and to help protect against dielectric breakdown across the edges of the specimens. The induced current was converted to a measurable voltage signal by means of a custom-built I–V converter, based on an operational amplifier in a 'virtual earth' configuration. Further details of the measurement system were given in a previous publication [10]. Numerical integration of the measured current with respect to time yielded the polarization, thereby enabling determination of the P–E characteristics of the material.

P–E measurements were conducted as a function of temperature by cooling from 150 °C to 30 °C under a continuous sinusoidal AC electric field with an amplitude of 2 kV mm^{-1} and a frequency of 20 Hz. P–E data were recorded at 10 °C intervals in order to provide an indication of the variation in remanent polarization P_r and saturation polarization P_s with temperature.

Ageing experiments were carried out by first thermally deageing the specimen at 150 °C for 1 hour. Subsequently, it was transferred to the oil bath, set at a temperature of 120 °C, and a continuous sinusoidal AC electric field was applied at an amplitude of 2 kV mm^{-1} and a frequency of 1 Hz. The oil bath was then cooled down to the required temperature

and allowed to stabilize for a period of at least 30 minutes. The ageing process was initiated by interrupting the continuous AC field and applying a single burst of two cycles at a field level of 2 kV mm^{-1}. This procedure acted to polarize the specimen in the negative sense, after which the resulting poled domain structure was progressively stabilized by the ageing processes.

Field dependent measurements were conducted at selected ageing times by applying single bursts of two sinusoidal voltage cycles at successively increasing field amplitudes from 0.1 to 2.0 kV mm^{-1}, in steps of 0.1 kV mm^{-1} and at a frequency of 20 Hz. These measurements were carried out to enable a detailed analysis of the field dependence of dielectric properties and internal bias field to be made.

For a linear, lossy dielectric represented by a complex permittivity ε_r^* we have

$$P^* \cong D^* = \varepsilon_0 \varepsilon_r^* E^* \tag{1}$$

where E^* represents the applied electric field, D^* the dielectric displacement and P^* the induced polarization. It is assumed in this expression that D^* and P^* are very nearly equal, which is true if $\varepsilon_r \gg 1$. Therefore, the magnitude of the complex permittivity $|\varepsilon_r^*|$ was determined by measuring the amplitude of the polarization waveform P_0 for a given field amplitude E_0.

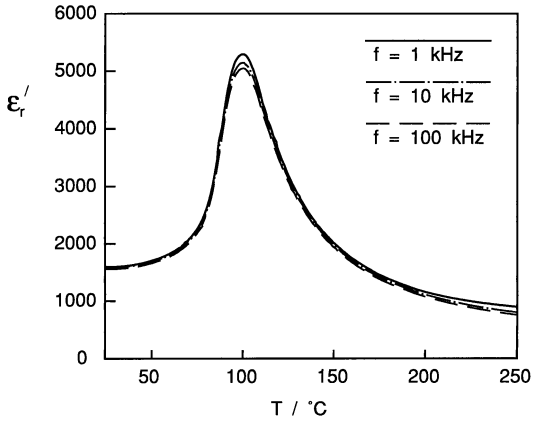

Figure 1. Temperature dependence of low-field dielectric permittivity.

The well known expression for the total power dissipated in a lossy capacitor is as follows [11]:

$$\text{power} = \tfrac{1}{2}\omega C U_0^2 \tan\delta \tag{2}$$

where ω = angular frequency, C = capacitance, U_0 = voltage amplitude and $\tan\delta$ = dielectric loss tangent. The dissipated power density can be written as

$$\frac{\text{power}}{\text{volume}} = \tfrac{1}{2}\omega \varepsilon_r'' E_0^2. \tag{3}$$

The hysteresis loss U_H represents the energy loss per cycle per unit volume and so we have an expression relating the measured value of U_H, calculated as the area of the P–E loop, to the imaginary part of dielectric permittivity ε_r'', as follows:

$$U_H = \pi \varepsilon_0 \varepsilon_r'' E_0^2. \tag{4}$$

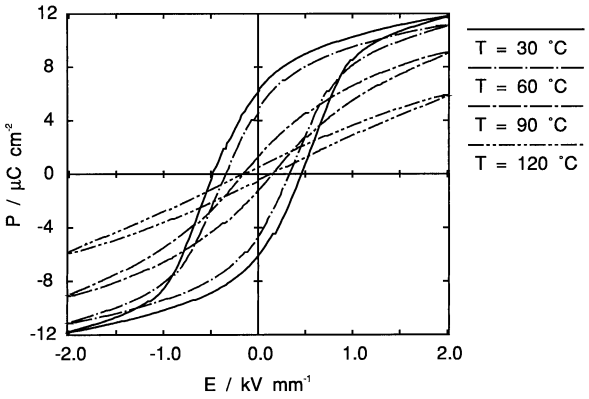

Figure 2. Change in high-field P–E characteristics as a function of temperature (E_0 = 2 kV mm^{-1}).

Subsequently, the real part of the permittivity ε_r' was found from these two values:

$$|\varepsilon_r^*| = \sqrt{(\varepsilon_r')^2 + (\varepsilon_r'')^2}. \tag{5}$$

It should be noted that this description of dielectric behaviour assumes a linear, lossy P–E relationship. As such, it cannot strictly be applied if a significant nonlinear component is present, as would be the case for a ferroelectric material subjected to a high electric field. In such a case, the ε_r' and ε_r'' values derived from the P–E data represent the equivalent or effective dielectric coefficients which give a measure of the total dielectric polarization and loss under a given set of measurement conditions.

3. Results

3.1. Temperature dependence of dielectric properties

Basic structural characterization procedures established that the material had a tetragonally distorted perovskite type crystal structure with a c/a ratio of 1.007 and a mean grain size (determined by the linear intercept method) of 4.1 μm. The absolute and relative densities were measured as 5.65 g cm^{-3} and 94% respectively.

It was evident from low-field dielectric measurements that the cubic (paraelectric) to tetragonal (ferroelectric) phase transition occurred at a Curie temperature of approximately 100 °C, as shown in figure 1. The peak in permittivity at the Curie point was relatively broad in comparison with pure $BaTiO_3$, suggesting a second-order ferroelectric phase transition rather than the first-order transition of the pure material. Alternatively, extrinsic factors such as chemical heterogeneity (for example) could have given rise to a distribution of Curie points, causing the observed diffuse phase transition. A slight frequency dependence of permittivity was also evident at the Curie point.

High-field P–E measurements indicated a near-linear P–E relationship at temperatures above 120 °C (figure 2). The presence of some hysteresis loss at high temperatures can be attributed to residual electronic conduction. Dielectric nonlinearity and hysteresis loss became increasingly evident at temperatures below 90 °C, corresponding to the appearance of the ferroelectric phase.

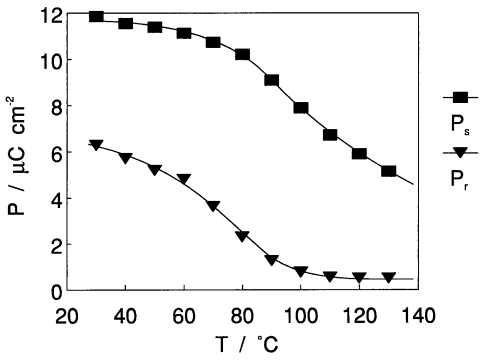

Figure 3. Temperature dependence of remanent and saturation polarization ($E_0 = 2$ kV mm^{-1}); lines are for guidance only.

Table 1. Frequency dependence of hysteresis loss U_H ($T = 120\,^{\circ}$C, $E_0 = 2.0$ kV mm^{-1}).

f (Hz)	U_H (kJ m^{-3})	Calculated resistivity ρ_{AC} (10^7 Ω m)
50	6.45	0.62
20.6	18.4	0.53
10.3	25.4	0.76
5.2	38.5	1.00
2.03	71.5	1.36
1.03	119	1.63

The measured variation of P_s and P_r as a function of temperature are presented in figure 3. It is apparent that P_r reduced gradually with increasing temperature, reaching a nearly constant value at 100 °C. This behaviour is consistent with the occurrence of a diffuse ferroelectric phase transition in this material, providing supporting evidence for the low-field dielectric measurements reported above.

The hysteresis loss at high temperatures increased significantly at lower measurement frequencies, supporting the view that it was due primarily to residual electronic conduction. For example, the values of U_H obtained at a temperature of 120 °C and at various measurement frequencies are given in table 1. If we assume that the high-temperature loss was due solely to electronic conduction, then we have

$$\varepsilon_r'' = \frac{\sigma_{AC}}{\omega\varepsilon_0} = \frac{1}{\omega\varepsilon_0\rho_{AC}} \tag{6}$$

where σ_{AC} and ρ_{AC} are the equivalent AC conductivity and resistivity respectively. By comparison with equation (4) above, we have

$$U_H = \frac{\pi E_0^2}{\omega\rho_{AC}}. \tag{7}$$

The data given in table 1 demonstrate an inverse dependence of U_H on frequency according to equation (7), yielding an equivalent AC resistivity ρ_{AC} of between 0.5×10^7 and 1.6×10^7 Ω m.

3.2. Field dependence of dielectric properties

At a temperature of 60 °C, the induced current waveform reflected the sinusoidal nature of the applied voltage signal for field levels below 0.6 kV mm^{-1}. A distortion of the current signal became increasingly apparent as the field amplitude increased; this developed into distinct peaks associated with ferroelectric polarization switching at high field levels. The transition from linear non-hysteretic to nonlinear hysteretic behaviour is demonstrated by the P–E curves presented in figure 4. It is clear from this figure that some degree of polarization switching began to occur at a field amplitude of approximately 0.8 kV mm^{-1} under this particular combination of measurement temperature and ageing time.

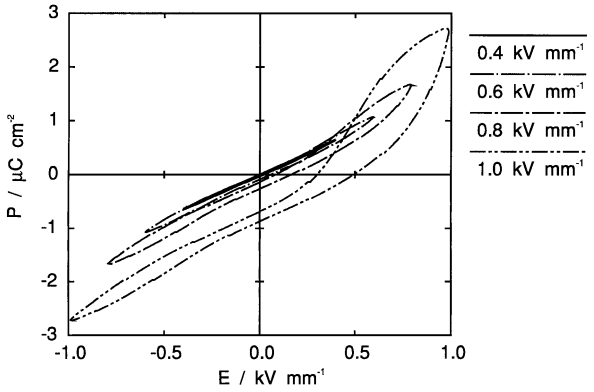

Figure 4. P–E loops obtained as a function of increasing field amplitude (T = 60 °C, ageing time = 25 h).

The dielectric coefficients ε_r' and ε_r'' derived from these P–E loops are presented in figure 5, which summarizes the results obtained at 60 °C for various ageing times. The general trend was an increase in both ε_r' and ε_r'' with increasing field amplitude. This observation has been attributed previously to the increasing domain wall contributions, as noted above [5–10]. For an ageing time of 25 hours, there were gradual increases in ε_r' and ε_r'' as a function of E_0 in the region $0.1 < E_0 < 0.7$ kV mm^{-1}, which covers the range of field strengths which are of most practical interest. The gradients of the ε_r'–E_0 and ε_r''–E_0 curves increased sharply beyond this 'threshold' field level, prior to saturation at 1.8 kV mm^{-1}. The equivalent $\tan\delta$ values obtained at various field levels and ageing times are summarized in table 2.

By comparison with the P–E loops presented in figure 4, it is evident that the changes in slope of the ε_r'–E_0 and ε_r''–E_0 curves are associated with the first occurrence of a significant contribution from ferroelectric polarization switching. The field strength at which this occurred was found to increase significantly as a function of ageing time, resulting in a pronounced shift of the curves to higher field strengths. Similar observations were made previously by Lewis [5] and Hagemann [6]. This effect can be related to domain stabilization processes due to acceptor ion-oxygen vacancy defect associates, as discussed by Robels and Arlt [12].

Dederichs and Arlt previously demonstrated how it is possible to distinguish between the ferroelectric domain wall and intrinsic ionic contributions to ε_r' by plotting a graph of ε_r' against ε_r'' during ageing at a given temperature [13]. Their method exploits the linear nature of the ε_r'–ε_r'' relationship, which arises if a single lossy polarization mechanism is

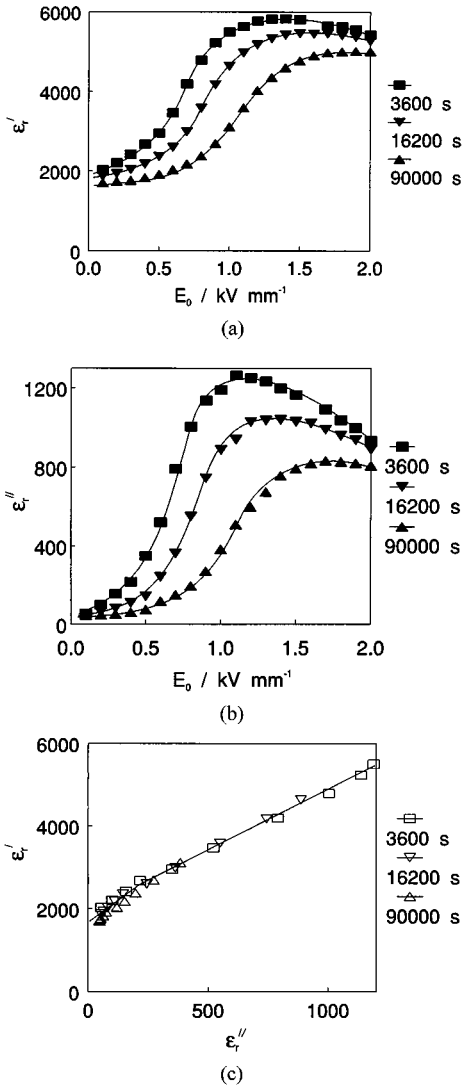

Figure 5. Field dependence of dielectric permittivity at various ageing times: (a) ε_r' against E_0; (b) ε_r'' against E_0; (c) ε_r' against ε_r'' ($T = 60\,^{\circ}$C); lines are for guidance only.

present. This method may be extended to describe the increasing ferroelectric domain wall contributions to ε_r' and ε_r'' as a function of field amplitude, as described in a previous publication [10]. In the present work, the data obtained at different ageing times appeared to lie on a common curve made up of two linear portions, as shown in figure 5(c). By comparison with the P–E data reported in figure 4(b), it is apparent that these two portions of the ε_r'–ε_r'' curve correspond to regimes within which either reversible (non-hysteretic) domain wall vibration or irreversible (hysteretic) domain switching effects dominate the lossy dielectric response. Therefore, it is possible in principle to distinguish between these two distinct domain-related polarization processes. The extrapolated intrinsic (loss-free) ε_r' value was approximately 1700.

Table 2. Representative $\tan\delta$ values obtained at 60 °C as a function of field amplitude and ageing time.

E_0 (kV mm^{-1})	$t = 1$ h	$t = 4.5$ h	$t = 25$ h
0.2	0.045	0.033	0.027
0.5	0.118	0.061	0.039
0.8	0.209	0.153	0.082
1.0	0.216	0.191	0.123
1.5	0.200	0.189	0.166
2.0	0.172	0.168	0.161

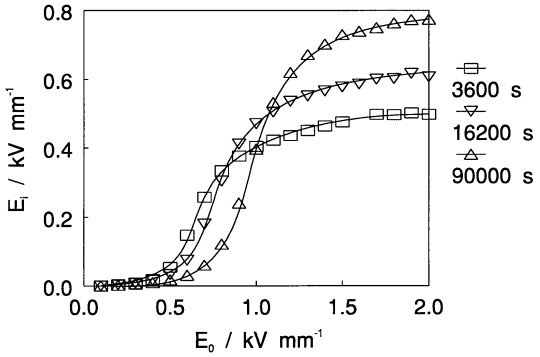

Figure 6. Variation of measured internal bias field as a function of field amplitude, at various ageing times ($T = 60$ °C); lines are for guidance only.

The ageing effects in acceptor-doped ferroelectrics are often described in terms of the macroscopic 'internal bias field' E_i, which is usually measured from the shift of the P–E loop along the electric field axis [14]. The value of E_i at a given ageing time represents the difficulty in switching the polarization in the direction opposite to that of the stabilized (aged) domain configuration, relative to that of re-polarization back to the stabilized state. This parameter is usually determined from P–E data measured at high field strengths approaching saturation. The present authors demonstrated previously that the apparent value of E_i is strongly dependent on the amplitude of the measuring field [15]. It is clear that at low field strengths, when no ferroelectric switching occurs, the measured value of E_i should be zero. As E_0 increases beyond a certain level, the degree of polarization switching should increase and so the apparent value of E_i should increase.

The results obtained for E_i in the present study verified the general argument presented above, as shown in figure 6. As expected, the value of E_i obtained at high field strengths increased significantly as a function of ageing time, from 0.50 kV mm^{-1} after 1 hour to 0.78 kV mm^{-1} after 25 hours, corresponding to an increased degree of ferroelectric domain stabilization. It is also interesting to note that the field level at which a significant internal bias field first appeared corresponded closely to the onset of ferroelectric polarization switching, as would be expected from the above argument. One consequence of this is that the apparent value of E_i actually *reduced* at longer ageing times if the amplitude of the measuring field was in the range $0.1 < E_0 < 1.0$ kV mm^{-1}. This effect can be understood by recognizing that the ageing processes increasingly restrict the ferroelectric domain switching in this intermediate-field region, giving rise to a more linear P–E relationship with an apparently smaller internal bias field.

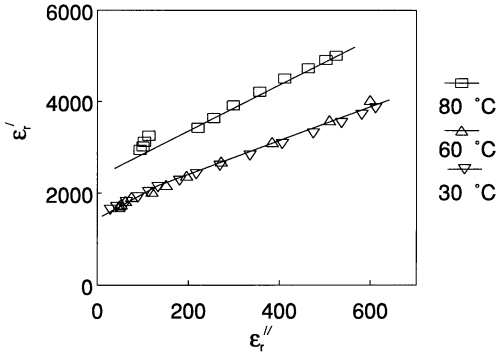

Figure 7. Field dependence of dielectric permittivity at various temperatures, plotted as ε_r' against ε_r'' (ageing time = 25 h); lines are for guidance only.

Table 3. Comparison of effective permittivity values recorded under continuous AC cycling and after ageing ($E_0 = 2.0$ kV mm^{-1}).

	Continuous cycling		Ageing time = 25 h	
T (°C)	ε_r'	ε_r''	ε_r'	ε_r''
30	6500	1500	4250	670
60	6180	1050	5020	810
80	5730	620	4780	520

The effect of temperature on the field dependence of permittivity was not as clear as that of the ageing time reported above. This was due in part to the effect of temperature on the ageing rate, which would have resulted in differing degrees of domain stabilization at a given ageing time. In general, the results obtained at 30 and 60 °C were similar, although the onset of ferroelectric polarization switching was more gradual at 30 °C (figure 7). The low-field ε_r' values were significantly higher at 80 °C, in accordance with the results presented in figure 1.

On the basis of the results presented in figure 3 above, it was anticipated that the high-field values of ε_r' and ε_r'' would increase at lower temperatures. However, such a clear trend was not observed. The equivalent ε_r' and ε_r'' values deduced from the data presented in figure 3, which were recorded under a continuous high AC field (i.e. without ageing), are listed in table 3 together with the values recorded after ageing for 25 hours. It is apparent that the ε_r' and ε_r'' values were reduced to a greater extent after ageing at the lower temperatures, resulting in a rather complex temperature dependence for the high-field data ($E_0 = 2$ kV mm^{-1}) recorded at a fixed ageing time.

The ε_r'–ε_r'' plot presented in figure 7 demonstrates the close similarity between the results obtained at 30 and 60 °C, which appear to follow a common curve with an extrapolated intrinsic ε_r' value of around 1600. The ε_r' values recorded at 80 °C were significantly higher with a slightly steeper gradient, indicating an intrinsic ionic permittivity of 2800.

The apparent internal bias field exhibited a predictable temperature dependence at low field levels, giving higher E_i values for higher measurement temperatures, as shown in figure 8. This trend reflects the enhanced degree of polarization switching at higher temperatures in the intermediate-field region ($0.1 < E_0 < 1.0$ kV mm^{-1}). The curves

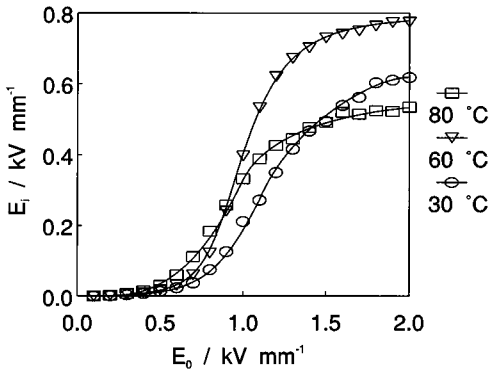

Figure 8. Variation of measured internal bias field as a function of field amplitude, at various ageing temperatures (ageing time = 25 h); lines are for guidance only.

started to cross over at higher field strengths, as the ferroelectric polarization switching was accomplished more completely at lower temperatures. At an ageing time of 25 hours, the high-field E_i values decreased in the order $E_i(60\,^{\circ}\mathrm{C}) > E_i(30\,^{\circ}\mathrm{C}) > E_i(80\,^{\circ}\mathrm{C})$. Previous authors established that the ultimate E_i values obtained in acceptor-doped $BaTiO_3$ ceramics are higher for lower ageing temperatures [16]. Therefore, it is anticipated that the values recorded at 30 °C would increase beyond those obtained at 60 °C for sufficiently long ageing times.

4. Discussion

The results presented in section 3.2 above demonstrate the field dependence of the complex dielectric permittivity of these materials as functions of ageing time and temperature. The changes in slope of the ε_r'–E_0, the ε_r''–E_0 and the ε_r'–ε_r'' relationships suggest that two distinct ferroelectric-domain-related polarization mechanisms contribute to the high-field dielectric coefficients. Visual inspection of the P–E 'sub-loops' presented in figure 4 reveal that these changes in slope are associated with a deviation from dielectric linearity and the occurrence of significant hysteresis. Therefore, the two extrinsic polarization mechanisms can be identified tentatively as ferroelectric domain wall vibration and domain switching; the former mechanism is assumed to contribute a linear lossy response, while the latter exhibits nonlinearity and hysteresis.

This observation is supported by measurements of the field dependence of the apparent internal bias field as functions of ageing time and temperature. The value of E_i in a poled material under a given combination of field amplitude and ageing time provides an indication of the extent of ferroelectric domain switching, as described above. The data presented in figures 6 and 8 show clearly the regimes of field amplitude, ageing time and temperature over which the internal bias field exhibits a significant non-zero value and therefore over which the domain switching contribution to the dielectric properties is expected to be significant. By comparison with the dielectric results presented in figures 5 and 7, a good correlation can be established between the appearance of the internal bias field and the ferroelectric domain switching mechanism.

In order to explore this argument further, an attempt was made to quantify the intrinsic, domain wall vibration and domain switching contributions to the induced polarization and

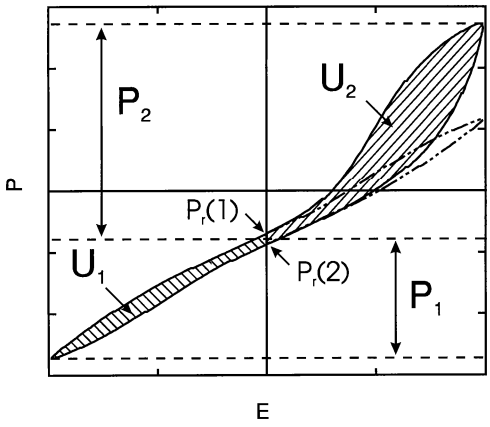

Figure 9. Definition of parameters P_1, P_2, U_1, U_2 from P–E hysteresis loop.

the effective dielectric properties. It was assumed for this procedure that the complex permittivity ε_r^* could be represented by contributions from these separate polarization mechanisms, denoted as ε_i (intrinsic), ε'_{dw} and ε''_{dw} (domain wall vibration) and ε'_{sw} and ε''_{sw} (domain switching). It is evident that the contributions from domain switching are nonlinear and hysteretic. Therefore, the values of ε'_{sw} and ε''_{sw} should be regarded as 'effective' dielectric coefficients, since by definition the complex dielectric permittivity is used as a means of describing lossy linear dielectric behaviour, as noted above. From a practical point of view, the 'effective' complex dielectric permittivity provides a measure of the total induced polarization and loss according to equations (1) to (3).

As a first step in the procedure, the form of a typical P–E 'sub-loop' was examined, as shown in figure 9. For this material, and under this particular set of measurement conditions, the application of an electric field in the negative sense (parallel to the stabilized polarization state) resulted in a predominantly linear lossy response, which can be attributed mainly to a combination of the intrinsic ionic polarization and that due to reversible domain wall vibration. In contrast, the application of an electric field in the positive sense (opposite to that of the stabilized polarization state) gave rise to an additional nonlinear contribution from ferroelectric domain switching.

A simple analysis procedure can be proposed under the assumption that the above description of the P–E characteristic is valid over the range of field strengths, ageing times and temperatures of interest. Clearly, this is not the case at high field levels ($E_0 \sim 2$ kV mm^{-1}) and/or short ageing times, as shown by the near-saturated P–E loops presented in figure 2. However, this does not present a major difficulty as long as the results obtained from this procedure are treated with consideration for the limitations of the model.

We can define the parameters P_1, P_2, U_1 and U_2 to represent the changes in polarization and hysteresis loss determined with respect to the negative and positive sides of the field axis respectively, as shown in figure 9. Assuming that the parameters P_1 and U_1 arise due to a combination of the intrinsic response and that due to reversible domain wall vibration, we can imagine this portion of the loop extending symmetrically to the positive side of the field axis (represented by the dashed curve), in which case we would have

$$\varepsilon''_{dw} = \frac{2U_1}{\pi \varepsilon_0 E_0^2}. \tag{8}$$

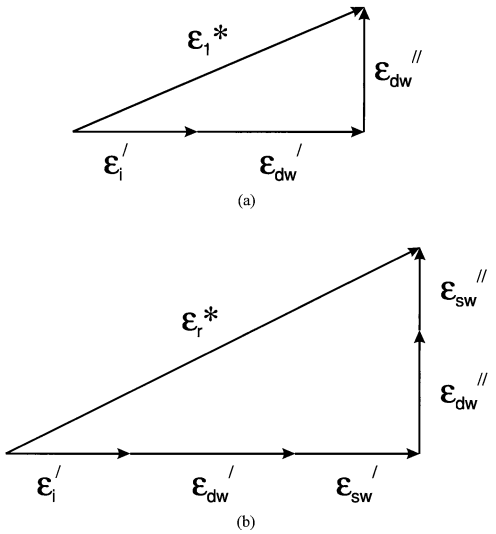

Figure 10. Contributions of intrinsic, domain wall vibration and domain switching mechanisms to measurable dielectric parameters (a) ε_1^* and (b) ε_r^*.

The sum of the intrinsic and domain wall contributions produces an induced polarization P_1^* with an equivalent permittivity of ε_1^*, as shown in figure 10(a). We have

$$\varepsilon_1^* = \frac{P_1^*}{\varepsilon_0 E_0} \tag{9}$$

and

$$|\varepsilon_1^*|^2 = (\varepsilon_i' + \varepsilon_{dw}')^2 + (\varepsilon_{dw}'')^2. \tag{10}$$

Therefore, ε_{dw}' may be determined from P_1 and the previously calculated value of ε_{dw}''.

A similar argument can be followed for the domain switching contributions to ε_r' and ε_r'', as illustrated in figure 10(b). This gives

$$\varepsilon_{sw}'' = \frac{U_2 - U_1}{\pi \varepsilon_0 E_0^2} \tag{11}$$

and

$$|\varepsilon_r^*|^2 = (\varepsilon_i' + \varepsilon_{dw}' + \varepsilon_{sw}')^2 + (\varepsilon_{dw}'' + \varepsilon_{sw}'')^2. \tag{12}$$

The results obtained by applying the procedure described above to the field dependent dielectric measurements are illustrated in figure 11. At a temperature of 60 °C and an ageing time of 1 h, the contributions from domain switching (ε_{sw}' and ε_{sw}'') were negligibly small for field levels below 0.5 kV mm^{-1}. In contrast, the reversible domain wall contributions (ε_{dw}' and ε_{dw}'') were most significant in this intermediate regime of field strengths. Furthermore, the values of ε_{dw}' and ε_{dw}'' increased significantly with increasing field amplitude up to 1 kV mm^{-1} (dependent on ageing time). It is clear that, once ferroelectric domain switching was initiated, this mechanism rapidly dominated the dielectric response, giving large increases in ε_{sw}' and ε_{sw}''.

The growth in ε_r' and ε_r'' as a function of field amplitude E_0 in ferroelectric ceramics has been discussed by previous authors in terms of an increase in the ferroelectric domain wall contributions, as noted above [5–10]. However, a detailed explanation for this phenomenon

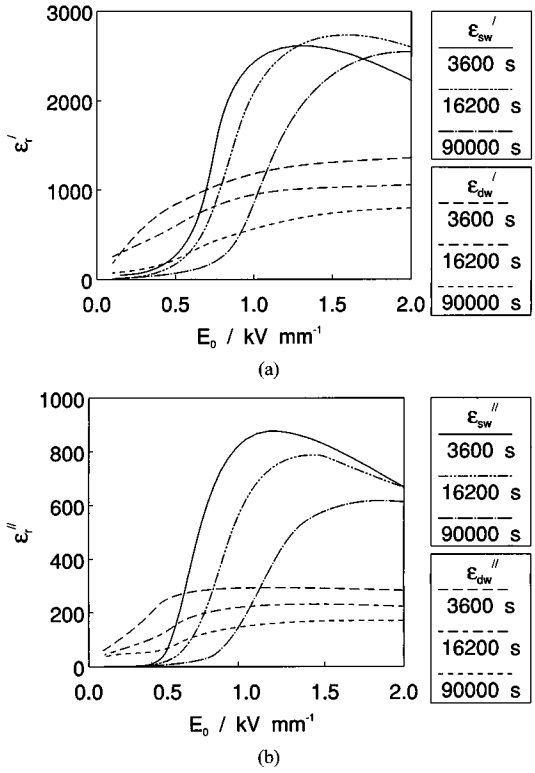

Figure 11. Separation of domain wall vibration and switching contributions to dielectric permittivity at various ageing times: (a) ε_r' against E_0; (b) ε_r'' against E_0 ($T = 60\,^{\circ}\mathrm{C}$); data points omitted for clarity.

is still lacking. In particular, the observed increases in the dielectric coefficients with E_0 seem to imply a reduction in the domain wall force constant k, defined by

$$k = \frac{F}{\Delta l} \tag{13}$$

where the domain wall is displaced by distance Δl due to force F [17].

Such a 'softening' of the force constant with increasing domain wall displacement is somewhat unexpected, since most nonlinear systems in nature tend to exhibit the opposite behaviour, as noted by Arlt [18]. As an alternative approach, he suggested that enhanced ferroelectric domain switching may be the prime cause of the observed increase in the dielectric coefficients. Similar conclusions were reached by Li *et al* [7] and Wu and Schulze [9]. Arlt identified a new type of domain wall, which could be nucleated on a grain boundary and subsequently propagate through the domain structure within the grain under the influence of the applied electric field, thereby reversing the average polarization of the grain [18].

A ferroelectric domain switching mechanism of this type may be responsible for the increases in ε_{sw}' and ε_{sw}'' described above (figure 11). However, the present results indicate that the non-hysteretic domain wall contributions ε_{dw}' and ε_{dw}'' also increase significantly with E_0. Therefore, a model is still required to explain the apparent softening of the domain wall force constant k with increasing wall displacement Δl. A localized 'pinning'

force may provide the correct explanation, if some of the defects responsible for domain stabilization become concentrated in the domain boundary region. The observation that the ferroelectric domain switching contribution to the dielectric coefficients is increasingly restricted during ageing indicates that a 'bulk' domain stabilization mechanism must also be present, in addition to any localized domain boundary effect.

As an alternative explanation for the apparent softening of the domain wall constant with increasing field amplitude, it is possible that some reversible domain switching may have occurred under the influence of the applied electric field, for example if the mechanism of domain switching involved gave rise to a significant associated elastic stress. On removal of the field, it would be expected that the elastic energy would be released, forcing the domain structure back to a state of lower residual stress. Further work will be required to enable a distinction to be made between these two different reversible polarization mechanisms.

Finally, it is interesting to compare the variations in E_i and the switched polarization P_{sw} as a function of E_0, where P_{sw} was calculated as $(P_0 - P_1)$. According to the interpretation of the observed increase in E_i as a function of E_0 outlined above, it might be expected that E_i and P_{sw} would exhibit a simple proportionality, since only those domains which are being switched at a given field amplitude would contribute to the measured value of E_i. However, in relative terms it was found that E_i initially increased more rapidly than P_{sw} as a function of E_0, as shown in figure 12. Similar results were obtained at various ageing times and temperatures.

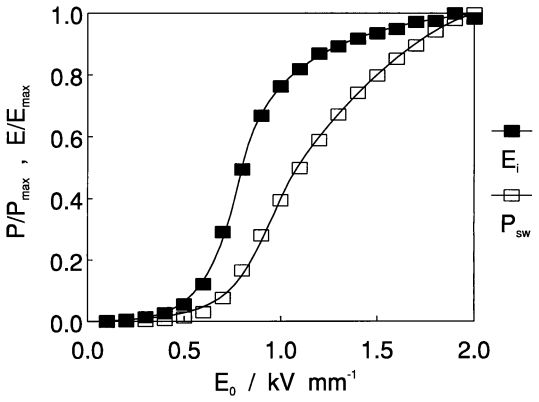

Figure 12. Comparison of variation in switched polarization and measured internal bias field as a function of field amplitude ($T = 60\,^{\circ}$C, ageing time = 25 h); lines are for guidance only.

Two possible explanations can be proposed to account for this behaviour. The most straightforward of these would involve statistical variations in E_i within different domains, due to an inhomogeneous distribution of the acceptor dopant or to variations in the grain clamping conditions. However, if such were the case it would be anticipated that P_{sw} would initially rise more rapidly than E_i, since those domains having a lower internal bias field would switch more easily at lower field levels. In fact, the opposite behaviour was observed in the present results (figure 12). Alternatively, this behaviour could arise due to the occurrence of a combination of different ferroelectric domain switching mechanisms, one of which (that having the higher associated coercive field) yielded effectively zero internal bias.

At present, it would be inappropriate to speculate further on the mechanisms of polarization reversal in this material, without supporting evidence (e.g. in the form of XRD or field-induced strain measurements). The domain switching model proposed by Arlt [18] provides a useful starting point in the search for a better description of the high-field dielectric behaviour of such materials.

5. Conclusions

Temperature dependent dielectric and high-field P–E measurements indicated the presence of a diffuse ferroelectric phase transition at a Curie temperature of approximately 100 °C. P–E measurements carried out as a function of field amplitude revealed a progression from a linear lossy response to nonlinear hysteretic behaviour. The equivalent dielectric coefficients ε_r' and ε_r'' derived from P–E loops exhibited a steep increase beyond a certain threshold field corresponding to the onset of significant nonlinearity and hysteresis. This threshold field was typically in the range 0.4 to 0.8 kV mm^{-1}, depending on ageing time and temperature.

Plotting the results on the complex permittivity plane yielded curves comprising two linear portions, indicating contributions from two distinct polarization mechanisms in addition to the intrinsic (loss-free) component. These were tentatively attributed to reversible ferroelectric domain wall motion and hysteretic domain switching. A procedure was proposed for determination of the individual contributions to the complex dielectric permittivity, based on the analysis of asymmetric P–E loops. The results obtained using this procedure showed significant increases in both the reversible domain wall vibration and hysteretic domain switching contributions as a function of increasing field amplitude, with the former being more prominent at field levels below 0.5 kV mm^{-1}.

The apparent internal bias field, determined from the shift of the P–E loop along the electric field axis, increased from 0 to 0.8 kV mm^{-1} as the field amplitude was incremented from 0.1 to 2.0 kV mm^{-1}. This behaviour was attributed to the increase in ferroelectric domain switching at higher field levels.

Acknowledgments

The authors would like to thank Morgan Matroc (Unilator Division) for supplying the ceramic powder and Mr G Ingham (Manchester Materials Science Centre) for technical assistance. Mr Ben-Omran acknowledges the financial support of Libyan Higher Education.

References

[1] Swartz S L 1990 Topics in electronic ceramics *IEEE Trans. Electr. Insul.* **EI-25** 935–87
[2] Morgan Matroc Unilator Division *Piezoelectric Ceramic Products*
[3] Butler J L, Rolt K D and Tito F A 1994 Piezoelectric ceramic mechanical and electrical stress study *J. Acoust. Soc. Am.* **96** 1914–17
[4] Von Hippel A 1950 Ferroelectricity, domain structure, and phase transitions of barium titanate *Rev. Mod. Phys.* **22** 221–37
[5] Lewis B 1960 Energy loss processes in ferroelectric ceramics *Proc. Phys. Soc.* **73** 17–24
[6] Hagemann H J 1978 Loss mechanisms and domain stabilisation in doped $BaTiO_3$ *J. Phys. C: Solid State Phys.* **11** 3333–44
[7] Li S, Cao W and Cross L E 1991 The extrinsic nature of nonlinear behaviour observed in lead zirconate titanate ferroelectric ceramic *J. Appl. Phys.* **69** 7219–24

[8] Robels U, Zadon Ch and Arlt G 1992 Linearization of dielectric nonlinearity by internal bias fields *Ferroelectrics* **133** 163–8
[9] Wu K and Schulze W A 1992 Effect of the ac field level on the aging of the dielectric response in polycrystalline $BaTiO_3$ *J. Am. Ceram. Soc.* **75** 3385–9
[10] Hall D A, Stevenson P J and Mullins T R 1997 Dielectric nonlinearity in hard piezoelectric ceramics *Br. Ceram. Proc.* **57** 197–211
[11] Moulson A J and Herbert J M 1990 *Electroceramics* (London: Chapman and Hall) pp 58–62
[12] Robels U and Arlt G 1993 Domain wall clamping by orientation of defects *J. Appl. Phys.* **73** 3454–56
[13] Dederichs H and Arlt G 1986 Aging of Fe-doped PZT ceramics and the domain wall contribution to the dielectric constant *Ferroelectrics* **68** 281–92
[14] Carl K and Hardtl K H 1978 Electrical after-effects in $Pb(Ti, Zr)O_3$ ceramics *Ferroelectrics* **17** 473–86
[15] Hall D A and Stevenson P J 1996 Field-induced destabilisation of hard PZT ceramics *Ferroelectrics* **187** 23–37
[16] Neumann H and Arlt G 1987 Dipole orientation in Cr-modified $BaTiO_3$ ceramics *Ferroelectrics* **76** 303–10
[17] Arlt G and Pertsev N A 1991 Force constant and the effective mass of 90° domain walls in ferroelectric ceramics *J. Appl. Phys.* **70** 2283–9
[18] Arlt G 1996 Switching and dielectric nonlinearity of ferroelectric ceramics *Ferroelectrics* **189** 91–101